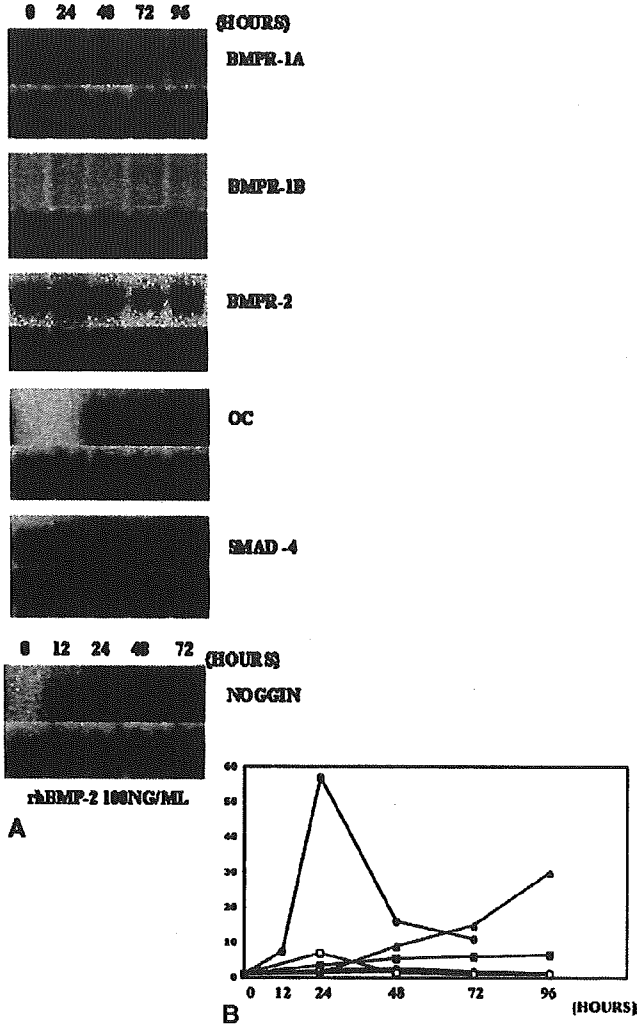

Fig. 3. Gene expression of BMPR-1A, -1B, -2, OC, and Smad-4 for 0, 24, 48, 72, and 96 h and Noggin for 0, 12, 24, 48, and 72 h after 100 ng/ml rhBMP-2 stimulation in muscle-derived primary culture cells by Northern blot analysis (**A**) and quantitation of the data of Northern blot analysis by Densitometry (**B**). G3PDH mRNA levels (*the bottoms of all lanes* are G3PDH) obtained by Northern blotting were used for normalization (**A**). The score on hour 0 (just after BMP stimulation) was used as a standard (**B**). After rhBMP-2 stimulation, OC was up-regulated time-dependently. Noggin level peaked at 24 h. Expression of BMPR-1A and -2 was increased moderately after 24 h, then gradually decreased thereafter. Smad-4 was gradually and weakly up-regulated after stimulation. BMPR-1B was not increased during the experimental period

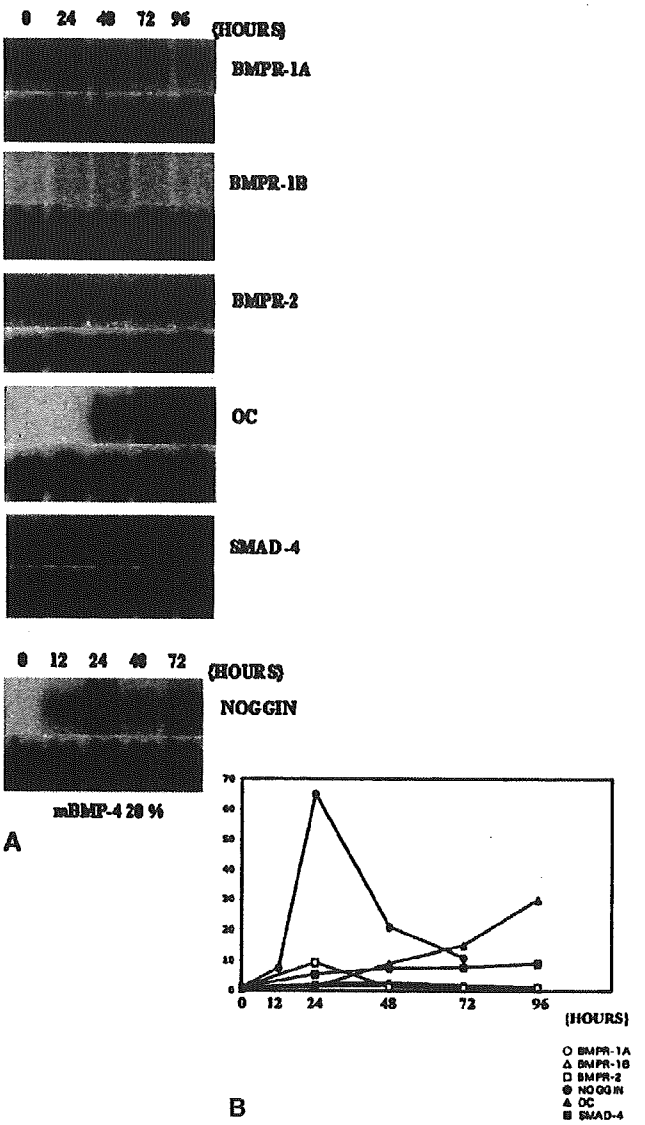

Fig. 4. Gene expression of BMPR-1A, -1B, -2, OC, and Smad-4 for 0, 24, 48, 72, and 96 h and Noggin for 0, 12, 24, 48, and 72 h after 20% mBMP-4 stimulation in muscle-derived primary culture cells by Northern blot analysis (**A**) and quantitation of the data of Northern blot analysis by Densitometry (**B**). G3PDH mRNA levels (*the bottoms of all lanes* are G3PDH) obtained by Northern blotting were used for normalization (**A**). The score on hour 0 (just after BMP stimulation) was used as a standard (**B**). The gene expression pattern of the molecules after stimulation of mBMP-4 (20%) was similar to that seen after stimulation of 100 ng/ml rhBMP-2

report using the pluripotent C2C12 cell line, and another study that revealed predominant expression of BMPR-1B in brain and not skeleton [20].

The induction of Noggin gene expression in cells of the osteoblastic lineage following exposure to rhBMP-2, and in fetal rat limb explants by BMP-7, has been reported [21,22]. In this study, Noggin gene expression was also confirmed in muscle-derived primary culture cells, an osteoblastic cell line (MC3T3-E1), and a nonosteoblastic, embryonic fibroblast-like cell line (NIH3T3) [16,23,24]. As Noggin is a representative antagonist of BMP action, the expression of Noggin might act as a negative regulator of the BMP-induced cellular reactions, and consequently reduce the susceptibility of the cells to BMPs.

Three classes of Smads, termed receptor-activated Smads (R-Smads), common Smads (Co-Smads), and inhibitory Smads (I-Smads), have been identified in mammals. Smads1, 5, and 8 are R-Smads that primarily mediate BMP signaling from the receptors to the nucleus [16,25]. Therefore, the up-regulation of Smad-4, which is a representative BMP signaling Co-Smad, in a time- or dose-

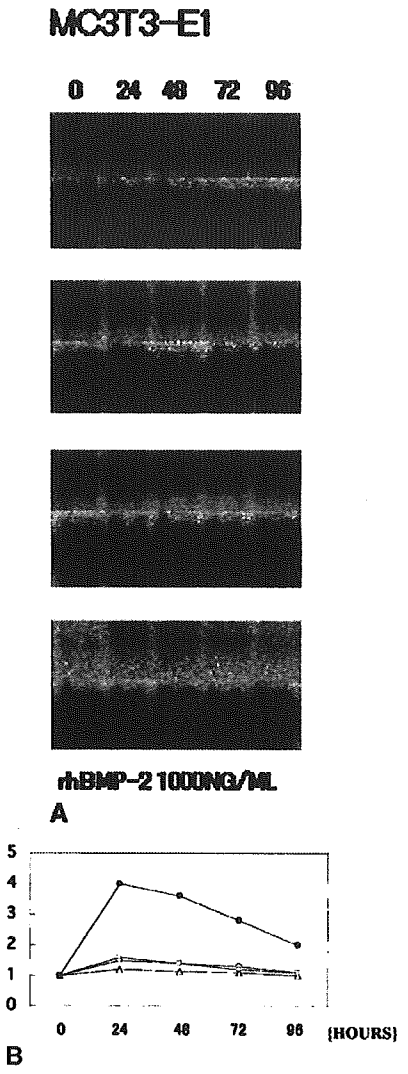

Fig. 5. Gene expression of BMPR-1A, -1B, -2, and Noggin for 0, 24, 48, 72, and 96 h after 1000 ng/ml rhBMP-2 stimulation in MC3T3-E1 cell line by Northern blot analysis (**A**) and quantitation of the data of Northern blot analysis by Densitometry (**B**). G3PDH mRNA levels (*the bottoms of all lanes* are G3PDH) obtained by Northern blotting were used for normalization (**A**). The score on hour 0 (just after BMP stimulation) was used as a standard (**B**). BMPR-1A and -2 were weakly induced after rhBMP-2 stimulation, peaked at 24 h, then decreased gradually. Noggin was also moderately induced after stimulation showed maximal expression at 24 h, then decreased thereafter. BMPR-1B was not induced during the course of the reaction

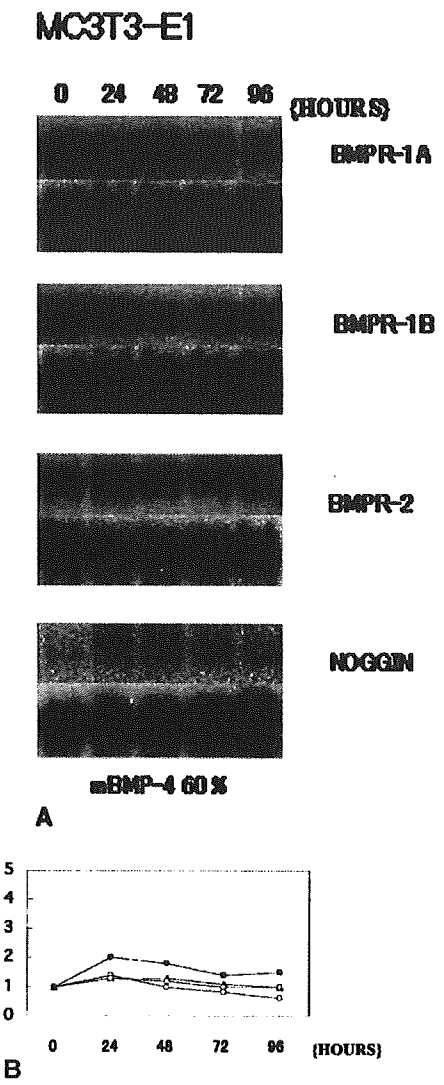

Fig. 6. Gene expression of BMPR-1A, -1B, -2, and Noggin for 0, 24, 48, 72, and 96 h after mBMP-4 (20%) stimulation in MC3T3-E1 cell line by Northern blot analysis (**A**) and quantitation of the data of Northern blot analysis by Densitometry (**B**). G3PDH mRNA levels (*the bottoms of all lanes* are G3PDH) obtained by Northern blotting were used for normalization (**A**). The score on hour 0 (just after BMP stimulation) was used as a standard (**B**). The gene expression pattern of the molecules after stimulation of mBMP-4 (20%) was similar to that seen after stimulation of 1000 ng/ml rhBMP-2, but the expression levels with mBMP-4 (20%) were smaller than those with 1000 ng/ml rhBMP-2

dependent manner suggests that BMP signaling in muscle tissue is regulated in a coordinated manner. OC is a well-characterized osteoblast differentiation marker, and MyoD is also a good marker for myoblastic differentiation [26]. Although the expression of MyoD was not detected in this study, the expression of OC was enhanced on day 2 after BMP-2 or -4 stimulation. These results indicate that BMP-induced osteogenic differentiation in muscle tissue might occur through a BMP/Smad signaling pathway, and muscle-derived primary culture cells might lose the muscle phenotype after BMP exposure.

The expression profiles were much more prominent for primary undifferentiated mesenchymal cells derived from muscle than for MC3T3-E1 or NIH3T3 cells in this study. Muscle-derived primary culture cells include a large population of undifferentiated mesenchymal cells, as described elsewhere [14]. Clearly, undifferentiated mesenchymal cells in muscle tissue are highly responsive to BMPs, based on

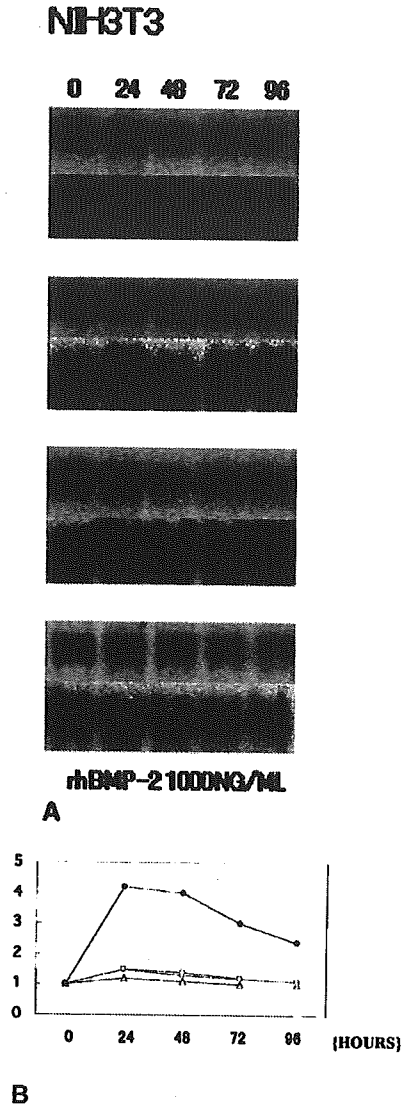

Fig. 7. Gene expression of BMPR-1A, -1B, -2, and Noggin for 0, 24, 48, 72, and 96 h after 1000 ng/ml rhBMP-2 stimulation in NIH3T3 cell line by Northern blot analysis (**A**) and quantitation of the data of Northern blot analysis by Densitometry (**B**). G3PDH mRNA levels (*the bottoms of all lanes* are G3PDH) obtained by Northern blotting were used for normalization (**A**). The score on hour 0 (just after BMP stimulation) was used as a standard (**B**). BMPR-1A and -2 were weakly induced after rhBMP-2 stimulation, peaked at 24 h, then decreased gradually. Noggin was moderately induced after stimulation showed maximal expression at 24 h, then decreased thereafter

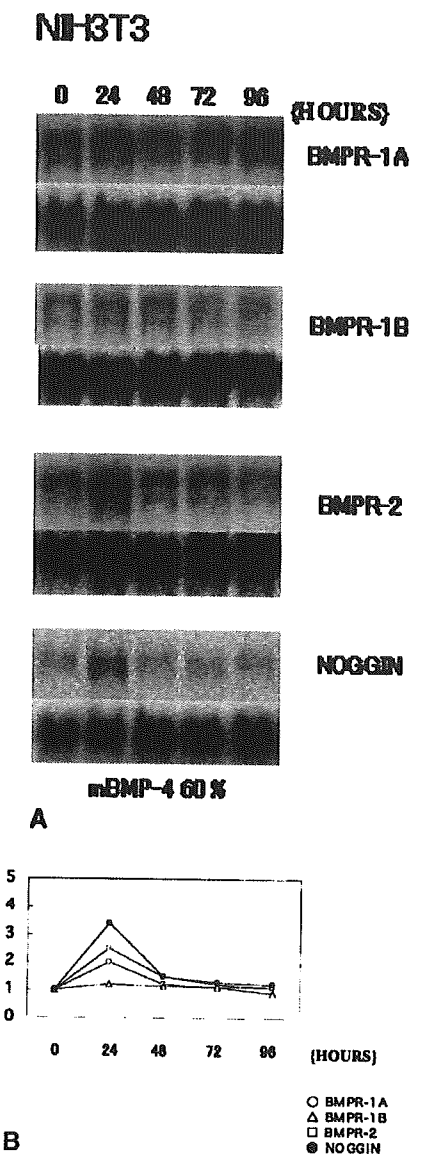

Fig. 8. Gene expression of BMPR-1A, -1B, -2, and Noggin for 0, 24, 48, 72, and 96 h after mBMP-4 (20%) stimulation in NIH3T3 cell line by Northern blot analysis (**A**) and quantitation of the data of Northern blot analysis by Densitometry (**B**). G3PDH mRNA levels (*the bottoms of all lanes* are G3PDH) obtained by Northern blotting were used for normalization (**A**). The score on hour 0 (just after BMP stimulation) was used as a standard (**B**). BMPR-1A and -2 were weakly induced after rhBMP-2 stimulation, peaked at 24 h, then decreased gradually. Noggin was moderately induced after stimulation showed maximal expression at 24 h, then decreased thereafter. BMPR-1B was not induced in all experimental stages. In NIH3T3 cells, the expression pattern was similar to that observed in the MC3T3-E1 culture experiments. Expression levels were greater in NIH3T3 cells than in MC3T3-E1 cells

the changes in gene and protein expression levels observed in this study. The proliferation and differentiation of osteoblasts from osteoprogenitor cells in murine bone marrow cultures induced by BMP-2 or -4 have been reported [27,28]. However, there have been few reports using muscle-derived primary culture cells with BMPs. In this study, the expression of BMP-related molecules was examined using undifferentiated mesenchymal cells derived from mouse muscle tissue.

The majority of undifferentiated mesenchymal cells in muscle-derived primary culture cells showed a fibroblastic appearance. These cells are considered to be heterogenous, and contain some kinds of precursor cells such as bone, cartilage, and muscle. They differentiate into each phenotype when they are placed in each differentiation condition.

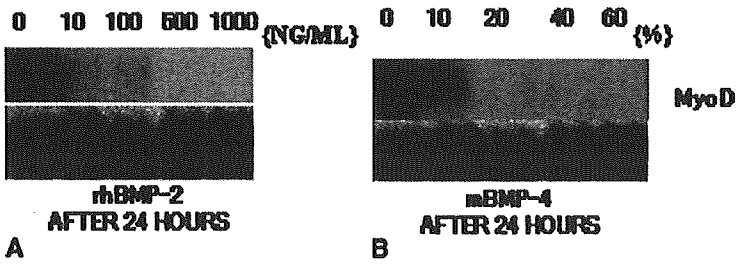

Fig. 9. The expression of MyoD in muscle-derived primary culture cells by Northern blot analyses. G3PDH mRNA levels obtained by Northern blotting were used for normalization. The expression of MyoD mRNA was not detected after BMP-2 or -4 exposure, and the expression was detected only at 0 and 24 h, and not after 24 h BMP stimulation

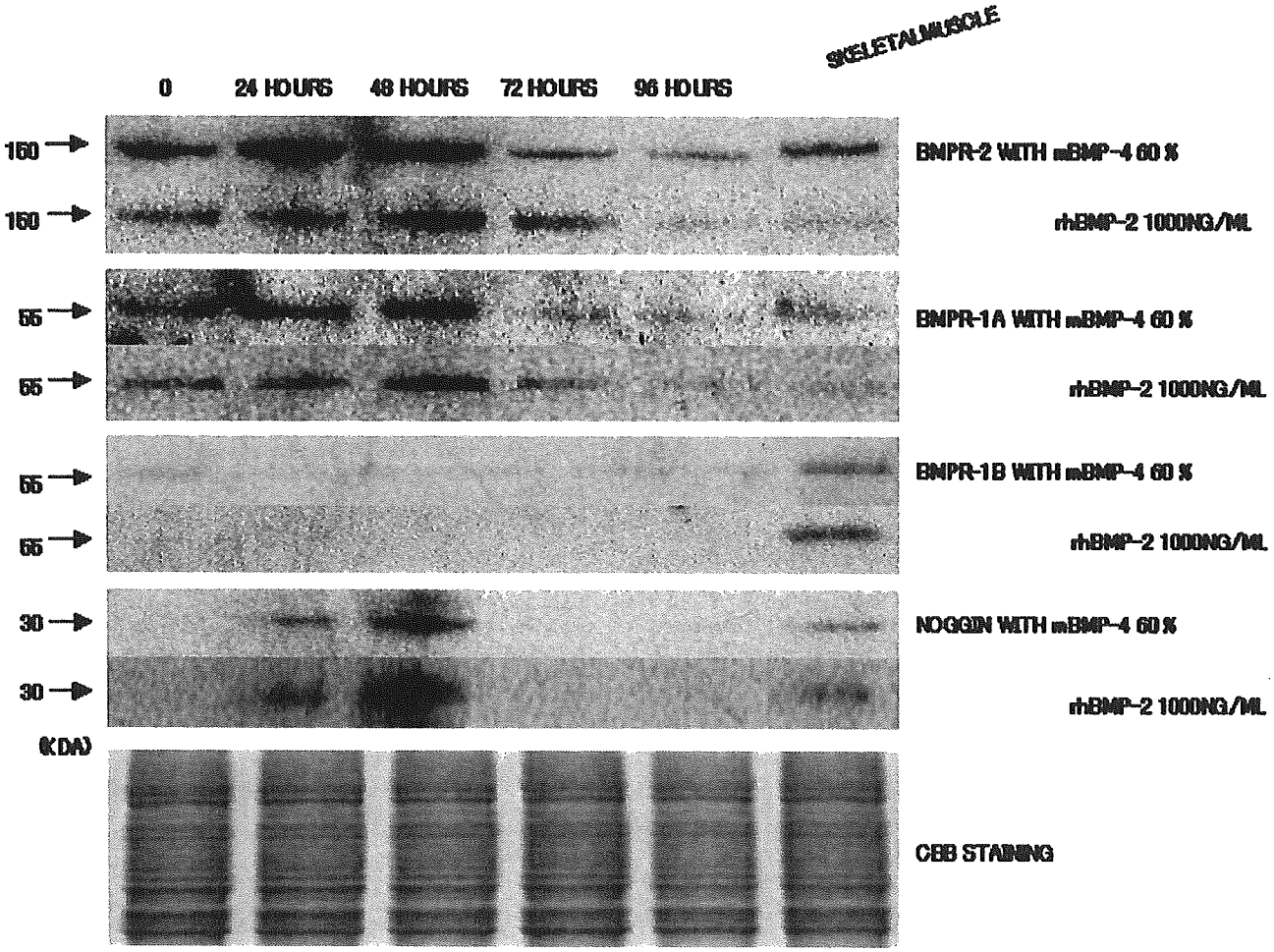

Fig. 10. Western blot analysis of BMPR-1A, -1B, -2, and Noggin after 60% mBMP-4 or 1000 ng/ml rhBMP-2 stimulation in muscle-derived primary culture cells. Equivalent loading and integrity of protein were confirmed by Coomassie brilliant blue staining on the gel (*lower panel*). Mouse skeletal muscle proteins were used as positive controls. BMPR-1A and -2 were detected at 0 h, induced at 24 h, peaked at 48 h, and then gradually decreased in both 60% mBMP-4 and 1000 ng/ml rhBMP-2 stimulation groups. Expression was greater for BMPR-2 than for BMPR-1A. BMPR-1B was not detectable during any stages in either treatment group. Noggin was not detected at 0 h, was up-regulated at 24 h, peaked at 48 h, and decreased thereafter

In our study, BMPs stimulated them to upregulate the expressions of a bone marker (OC) and cartilage markers (type II collagen and aggrecan, data not shown), but not the muscle marker examined previously. However, it is unclear whether bone and cartilage phenotypes were induced by BMPs in separate cells or in a single cell.

To further understand the potential autoregulatory mechanism in response to BMP, further gene expression

studies will be necessary. Ultimately, this knowledge may provide new approaches to the regulation of local and systemic bone formation.

References

1. Aspenberg P, Turek T (1996) BMP-2 for intramuscular bone induction: effect in squirrel monkeys is dependent on implantation site. Acta Orthop Scand 67:3–6
2. Itoh H, Ebara S, Kamimura M, Tateiwa Y, Kinoshita T, Yuzawa Y, Takaoka K (1999) Experimental spinal fusion with use of recombinant human bone morphogenetic protein. 2. Spine 24:1402–405
3. Takaoka K, Yoshikawa H, Hashimoto J, Ono K, Matsui M, Nakazato H (1994) Transfilter bone induction by Chinese hamster ovary (CHO) cells transfected by DNA encoding bone morphogenetic protein-4. Clin Orthop 300:269–273
4. Kaplan FS, Shore EM (1999) Illustrative disorders of ectopic skeletal morphogenesis: a childhood parallax for studies in gravitational and space biology. Gravit Space Biol Bull 12:27–38
5. Miyazono K, Ichijo H, Heldin CH (1993) Transforming growth factor-beta: latent forms, binding proteins and receptors. Growth Factors 8:11–22
6. Fujii M, Takeda K, Imamura T, Aoki H, Sampath TK, et al. (1999) Roles of bone morphogenetic protein type I receptors and Smad proteins in osteoblast and chondroblast differentiation. Mol Biol Cell 10:3801–3813
7. Ishidou Y, Kitajima I, Obama H, Maruyama I, Murata F, et al. (1995) Enhanced expression of type I receptors for bone morphogenetic proteins during bone formation. J Bone Miner Res 10: 1651–1659
8. Onishi T, Ishidou Y, Nagamine T, Yone K, Iamamura T, et al. (1998) Distinct and overlapping patterns of localization of bone morphogenetic protein (BMP) family members and a BMP type II receptor during fracture healing in rats. Bone 22:605–612
9. Kaneko H, Arakawa T, Mano H, Kaneda T, Ogasawara A, et al. (2000) Direct stimulation of osteoclastic bone resorption by bone morphogenetic protein (BMP)-2 and expression of BMP receptors in mature osteoclasts. Bone 27:479–486
10. Nakamura Y, Wakitani S, Nakayama J, Wakabayashi S, Horiuchi H, Takaoka K (2003) Temporal and spatial expression profiles of BMP receptors and Noggin during BMP-2-induced ectopic bone formation. J Bone Miner Res 18:1854–1862
11. Horiuchi H, Saito N, Kinoshita T, Wakabayashi S, Tsutsumimoto T, Takaoka K (2001) Enhancement of bone morphogenetic protein-2-induced new bone formation in mice by the phosphodiesterase inhibitor pentoxifylline. Bone 28:290–294
12. Takaoka K, Yoshikawa H, Hashimoto J, Ono K, Matsui M, Nakazato H (1994) Transfilter bone induction by Chinese hamster ovary (CHO) cells transfected by DNA encoding bone morphogenetic protein-4. Clin Orthop 300:269–273
13. Tsutsumimoto T, Wakabayashi S, Kinoshita T, Horiuchi H, Takaoka K (2002) A phosphodiesterase inhibitor, pentoxifylline, enhances the bone morphogenetic protein-4 (BMP-4)-dependent differentiation of osteoprogenitor cells. Bone 31:396–401
14. Yaffe D (1973) Rat skeletal muscle cells. In: Kruse PF, Patterson MK (eds) Tissue Culture, vol 16. Academic Press, New York, p 106–114
15. Yoshimura Y, Nomura S, Kawasaki S, Tsutsumimoto T, Shimizu T, Takaoka K (2001) Colocalization of Noggin and bone morphogenetic protein-4 during fracture healing. J Bone Miner Res 16:876–884
16. Kamiya N, Jikko A, Kimata K, Damsky C, Shimizu K, Watanabe H (2002) Establishment of a novel chondrocytic cell line N1511 derived from p53-null mice. J Bone Miner Res 17:1832–1842
17. Jiao K, Zhou Y, Hogan BL (2002) Identification of mZnf8, a mouse Kruppel-like transcriptional repressor, as a novel nuclear interaction partner of Smad1. Mol Cell Biol 22:7633–7644
18. Yamaguchi A, Ishizuya T, Kitou N, Wada Y, Katagiri T, et al. (1996) Effects of BMP-2, BMP-4, and BMP-6 on osteoblastic differentiation of bone marrow-derived stromal cell lines, ST2 and MC3T3-G2/PA6. Biochem Biophys Res Commun 220:366–371
19. Zhao M, Harris SE, Horn D, Geng Z, Nishimura R, Mundy GR, Chen D (2002) Bone morphogenetic protein receptor signaling is necessary for normal murine postnatal bone formation. J Cell Biol 157:1049–1060
20. Wlodarski KH, Reddi AH (1986) Importance of skeletal muscle environment for ectopic bone induction in mice. Folia Biol (Krakow) 34:425–434
21. Chen D, Ji X, Harris MA, Feng JQ, Karsenty G, et al. (1998) Differential roles for bone morphogenetic protein (BMP) receptor type 1B and 1A in differentiation and specification of mesenchymal precursor cells to osteoblast and adipocyte lineages. J Cell Biol 142:295–305
22. Akiyama S, Katagiri T, Namiki M, Yamaji N, Yamamoto N, et al. (1997) Constitutively active BMP type I receptors transduce BMP-2 signals without the ligand in C2C12 myoblasts. Exp Cell Res 235:362–369
23. Gazzerro E, Gangji V, Canalis E (1998) Bone morphogenetic proteins induce the expression of Noggin, which limits their activity in cultured rat osteoblasts. J Clin Invest 15:2106–2114
24. Nifuji A, Noda M (1999) Coordinated expression of Noggin and bone morphogenetic proteins (BMPs) during early skeletogenesis and induction of Noggin expression by BMP-7. J Bone Miner Res 14:2057–2066
25. Attisano L, Tuen Lee-Hoeflich S (2001) The Smads Genome. Biol 2:Reviews3010
26. Yamamoto N, Akiyama S, Katagiri T, Namiki M, Kurosawa T, Suda T (1997) Smad1 and smad5 act downstream of intracellular signalings of BMP-2 that inhibits myogenic differentiation and induces osteoblast differentiation in C2C12 myoblasts. Biochem Biophys Res Commun 238:574–580
27. Zou H, Wieser R, Massague J, Niswander L (1997) Distinct roles of type I bone morphogenetic protein receptors in the formation and differentiation of cartilage. Genes Dev 11:2191–2203
28. Abe E, Yamamoto M, Taguchi Y, Lecka-Czernik B, O'Brien CA, et al. (2000) Essential requirement of BMPs-2/4 for both osteoblast and osteoclast formation in murine bone marrow cultures from adult mice: antagonism by Noggin. J Bone Miner Res 15:663–673

ARTHRITIS & RHEUMATISM
Vol. 52, No. 2, February 2005, pp 637–641
DOI 10.1002/art.20794

Use of Local Electroporation Enhances Methotrexate Effects With Minimum Dose in Adjuvant-Induced Arthritis

Masahiro Tada, Kentaro Inui, Tatsuya Koike, and Kunio Takaoka

Objective. **To investigate the effects of electrical pulses on the ability of methotrexate (MTX) to attenuate inflammation and subsequent joint destruction in rats with adjuvant-induced arthritis (AIA).**

Methods. **Rats in the experimental group received an intraperitoneal injection of MTX (0.125 mg/kg body weight), followed 30 minutes later by application of direct electrical pulses (50V, 8 Hz) to their left hind paws with an electroporation apparatus (M+/E+ group; n = 8). The procedure was repeated twice weekly for 3 weeks. Three control groups received the following treatments, respectively: MTX without electrical treatment (M+/E− group; n = 9), electrical treatment but no MTX (M−/E+ group; n = 10), or no electrical treatment and no MTX (M−/E− group; n = 9). Progression of AIA was monitored by joint swelling and radiologic and histologic changes in the ankle joint.**

Results. **Three weeks after injection of the adjuvant, and at the height of the arthritic reaction, the swelling and radiologic and histologic changes in the left hind paws in the M+/E+ rats were significantly reduced, as compared with changes observed in the control groups.**

Conclusion. **These results demonstrate that application of electrical pulses in combination with use of systemic low-dose MTX can ameliorate local arthritic reactions. This response probably occurs because electrical stimulation promotes transient passage of MTX through pores in the cell membranes, with a resultant local increase in the concentration of the drug within the cells. These results point to a potential use of electrochemotherapy to increase the efficacy of MTX or other drugs in an arthritic joint that is refractory to treatment, without increasing the dose of the drug.**

Although new biologic agents (1) can ameliorate inflammatory reactions and consequently protect the joints of patients with rheumatoid disease from progressive damage (2), methotrexate (MTX) remains one of the most effective and widely used disease-modifying antirheumatic drugs (DMARDs) (3). However, chronic inflammation often persists in isolated joints even after effective systemic MTX treatment, presumably as a result of an inadequate concentration of MTX in the joint that is refractory to treatment. In patients with persistent inflammation, synovectomy is often indicated for symptomatic relief, although data on the long-term clinical effectiveness of this approach are limited (4). Another option is an additional dose of MTX, but this increases the risk of adverse events. Because MTX has weak cell permeability, and the pharmacologic effects of this drug depend upon its intracellular concentration, any method for increasing intracellular MTX levels in the joint may be effective in attenuating the inflammatory response.

Electroporation has been used to facilitate the transport of nonpermeable molecules into cells. Transient cell membrane pores, generated electrically, allow nonpermeable molecules, including genes and drugs, to enter into the cells (5). Electroporation systems are now available for clinical use to deliver anticancer drugs into malignant solid tumor cells (6–8) as electrochemotherapy. Encouraging clinical results have been reported for the treatment of malignancies, in terms of efficacy, safety, and cost (9). This suggests that electroporation may be useful for the local treatment of rheumatoid arthritis (RA) that is refractory to conventional therapy.

We used electroporation to enhance the effect of

Supported by the Ministry of Education, Culture, Sports, Science and Technology of Japan (grant-in-aid 15591594).

Masahiro Tada, MD, Kentaro Inui, MD, PhD, Tatsuya Koike, MD, PhD, Kunio Takaoka, MD, PhD: Osaka City University, Graduate School of Medicine, Osaka, Japan.

Address correspondence and reprint requests to Masahiro Tada, MD, Department of Orthopaedic Surgery, Osaka City University, Graduate School of Medicine, 1-4-3 Asahimachi, Abeno-ku, Osaka 545-8585, Japan. E-mail: m-tada@med.osaka-cu.ac.jp.

Submitted for publication May 11, 2004; accepted in revised form October 21, 2004.

low-dose MTX treatment on the progression to severe arthritis and associated joint destruction in a rat model of adjuvant-induced arthritis (AIA) (10–12).

MATERIALS AND METHODS

Animals. Inbred 7-week-old male Lewis rats were purchased from Charles River Japan (Kanagawa, Japan) and housed with free access to standard laboratory chow and water, under 12-hour dark/light cycles in conditioned air.

Induction of arthritis. The adjuvant mixture was prepared by mixing dried heat-killed *Mycobacterium butyricum* (Difco, Detroit, MI) in paraffin oil (Wako, Tokyo, Japan) at a concentration of 5 mg/ml. To induce systemic arthritis, 0.2 ml of the preparation was injected into the tail bases of 8-week-old rats that had received anesthesia via ethyl ether inhalation.

Pulsed electrical stimulation for electroporation. For electrical stimulation to generate transient pores in cell membranes at the target tissue site, we used an electroporation apparatus (CUY-21; Gene System, Osaka, Japan). Direct-current electrical pulses (8 Hz, 75 msec pulse duration, 50 volts/cm electrode distance) of 1-second duration were delivered 6 times during a single procedure. Each of the six 1-second pulses was applied by 2 parallel stainless steel electrodes that were moved between each pulse through 60° in a plane perpendicular to the long axis of the left hind paws, 30 minutes after an intraperitoneal injection of MTX or saline. We used electrode paste (Gelaid; Nihon Koden, Tokyo, Japan) to prevent skin burns.

Experimental protocol. The animals were assigned to an experimental group or to 1 of 3 control groups, as follows: MTX injection with electroporation (M+/E+ [experimental] group; n = 8), MTX without electroporation (M+/E− group; n = 9), electroporation with saline (M−/E+ group; n = 10), or no treatment (M−/E− group; n = 9).

MTX was provided by Wyeth-Pharmaceutical (Tokyo, Japan). The dose of MTX was set to 0.125 mg/kg body weight, based on preliminary experimental data indicating that no significant systemic antiarthritic changes were recognized at this dose. The drug was administered intraperitoneally twice weekly for 3 weeks, and the animals were killed by asphyxia in carbon dioxide (for radiologic and histologic examination).

These experimental protocols were in accordance with institutional regulations for animal care and were approved by the Institutional Committee for Animal Care of Osaka City University.

Gross inspection and radiologic evaluation. Twice weekly, the animals were weighed using an electronic balance, and hind paw thickness was measured with digital calipers. Three weeks after the adjuvant was injected, the animals were killed using CO_2 asphyxiation, and both hind limbs were harvested and fixed by perfusing cold 4% paraformaldehyde through the left ventricle, followed by immersion in cold 4% paraformaldehyde solution. Soft x-ray images of the hind paws were obtained with a soft x-ray apparatus (DCS-600EX; Aloka, Tokyo, Japan) using settings of 45 kV, 4 mA, and 30 seconds of exposure time. Destructive changes in hind paw bones seen on radiographs were evaluated by criteria previously described by Clark et al (13), with some modifications. Briefly, radiographic

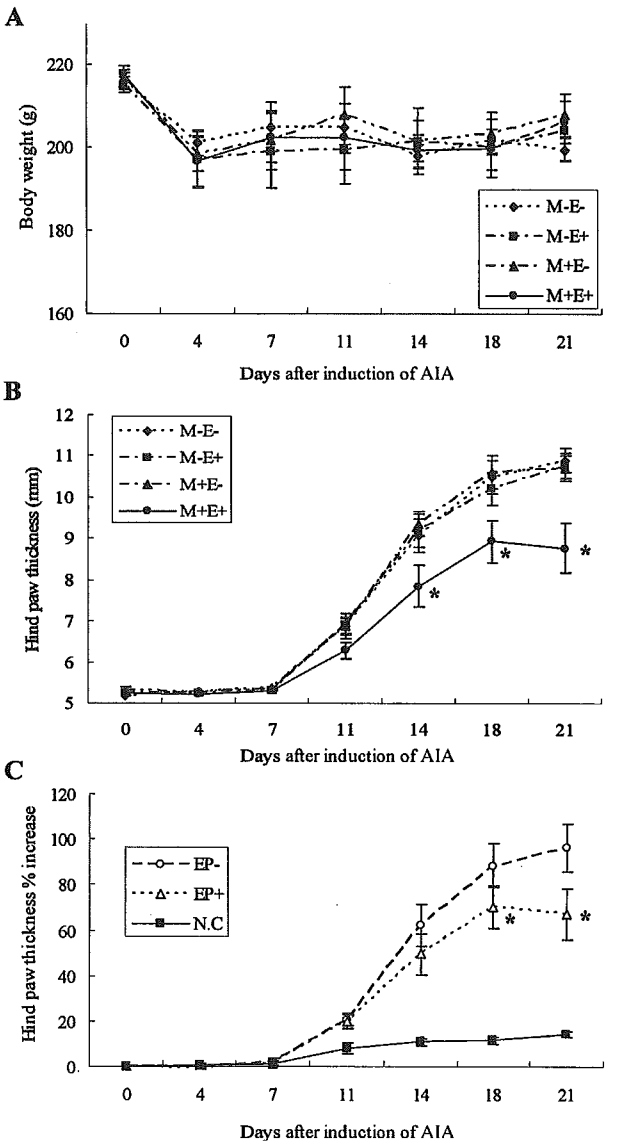

Figure 1. Effects of electrochemotherapy with methotrexate (MTX) on body weight and paw swelling in rats with adjuvant-induced arthritis (AIA). **A,** Weight loss was observed in all groups on day 4. There was no significant weight difference between the 4 groups throughout the entire study period. **B,** Left hind paw thickness, as measured by digital calipers, was maximal on day 21 in the M−/E− (no treatment; n = 9), M−/E+ (electroporation with saline; n = 10), and M+/E− (MTX without electroporation; n = 9) groups. The thickness of the left hind paw treated with electrical pulses after administration of MTX, 0.125 mg/kg/week (M+/E+; n = 8) was significantly decreased when compared with the other groups. * = $P < 0.05$ versus the M−/E−, M−/E+, and M+/E− groups. **C,** Effects of electrical pulses on paw swelling in the M+/E+ group. Electrical pulses were applied to the left hind paw only (electrically treated [EP+]) (n = 8), not the right paw (not electrically treated [EP−]) (n = 8). Application of electrical pulses after administration of low-dose MTX significantly inhibited hind paw swelling on days 18 and 21, as assessed by paw thickness and when compared with EP− paws. NC = negative control (non–adjuvant-injected model) (n = 5). * = $P < 0.05$ versus EP−. Bars show the mean ± SEM.

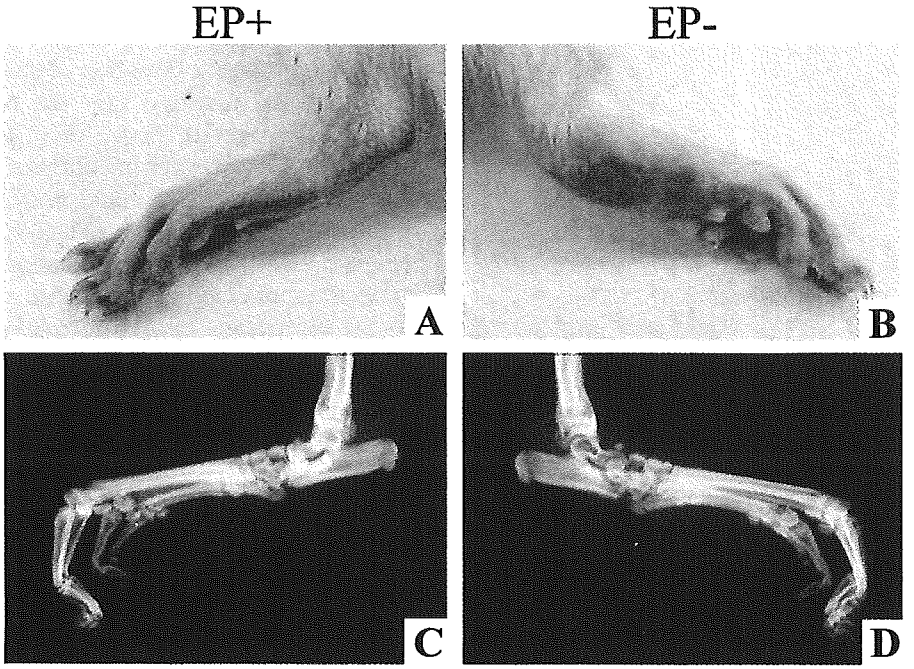

Figure 2. Gross appearance and radiographs of the hind paws of the same rat in the M+/E+ group on day 21. Following administration of MTX (0.125 mg/kg/week), electrical pulses were applied to the left hind paw only (EP+) (**A** and **C**). Note the obvious difference in the degree of swelling and joint damage between the left paw (EP+) and right paw (EP−) in gross appearance (**A** and **B**), as well as on soft x-ray (**C** and **D**). See Figure 1 for definitions.

changes in terms of radiodensity, subchondral bone erosion, periosteal reaction, and cartilage space were evaluated under blinded conditions by 2 rheumatologists (KI and TK) and graded on a 0–3 scale (where 0 = normal and 3 = severely damaged).

Histologic sections. Both hind paws were harvested from the animals for histopathologic examination. After the removal of skin, bones in the hind paws were decalcified in a neutral buffered 14% solution of EDTA/10% formalin, dehydrated in a graded ethanol series, embedded in paraffin, sectioned sagittally into 4-μm sections, and stained with hematoxylin and eosin or toluidine blue. Pathologic changes were evaluated by 2 observers according to a previously reported rating system (14), as follows: grade 0 = normal synovium, cartilage, and bone; grade 1 = hypertrophic synovium with cellular infiltration without pathologic change in bone and cartilage; grade 2 = pannus formation and cartilage erosion in addition to the hypertrophic synovium; grade 3 = additional severe erosion of cartilage and subchondral bone; grade 4 = loss of joint integrity and ankylosis.

In order to identify and count osteoclastic cells, sections were stained for tartrate-resistant acid phosphate (TRAP) using a staining kit (Sigma-Aldrich, St. Louis, MO). TRAP-positive multinucleated cells were counted in 11 selected fields (8 fields in the distal tibia and 3 fields in the talus), all at 100× magnification.

Statistical analysis. Body weight and hind paw thickness were evaluated by repeated analysis of variance and Fisher's protected least significant difference test. Pairwise comparisons were made using Wilcoxon's signed rank tests among groups. All statistical analyses were carried out using StatView software version 5.0 (SAS Institute, Cary, NC). *P* values less than or equal to 0.05 were considered significant.

RESULTS

Effects of electrochemotherapy on progression of AIA. No significant difference in body weight was noted between the 4 groups during the course of this experiment (Figure 1A), indicating that low-dose MTX, with or without electroporation, had little effect on the systemic physical condition of the rats with AIA.

The thickness of the hind paws in all rats was

Table 1. Radiologic and histologic scores and osteoclast numbers in rat AIA, 21 days after injection of adjuvant*

Group	Radiologic score (n = 8)	Histologic score (n = 8)	Osteoclast number (n = 5)
Right hind paw, EP-negative	3.8 ± 4.5	2.5 ± 1.2	77.6 ± 10.2
Left hind paw, EP-positive†	1.8 ± 2.2	1.3 ± 0.5	22.0 ± 2.4

* Values are the mean ± SD. AIA = adjuvant-induced arthritis; EP = electroporation.
† For all comparisons, $P < 0.05$ versus EP-negative.

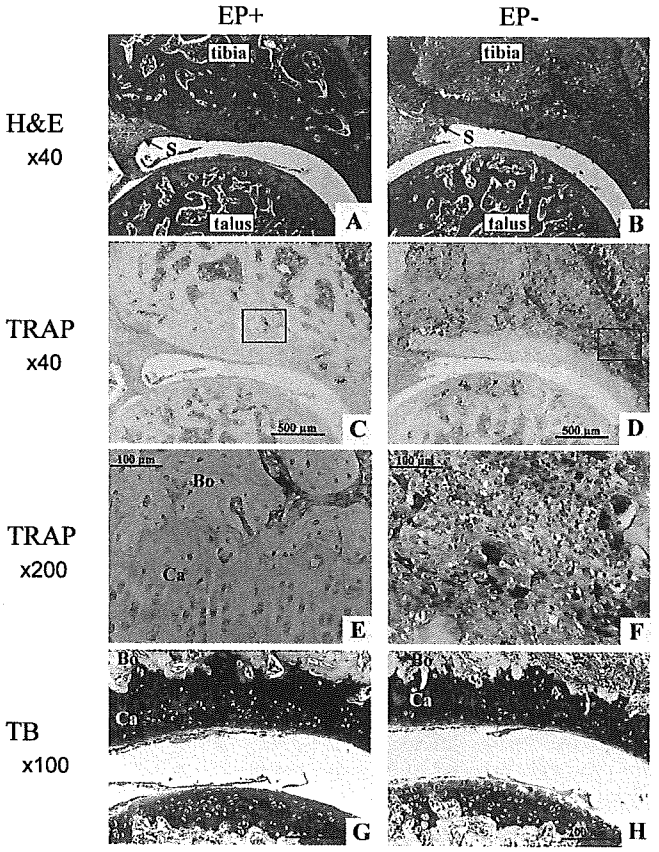

Figure 3. Histologic analysis of the ankle joints of the same rat in the M+/E+ group on day 21. **A** and **B,** Staining with hematoxylin and eosin (H&E). **C, D, E,** and **F,** Staining with tartrate-resistant acid phosphate (TRAP). **G** and **H,** Staining with toluidine blue (TB). The electroporation procedure was applied to the left ankle joint only (EP+) (**A, C, E,** and **G**). No inflammatory synovial tissue erosion into subchondral bone was observed with application of electroporation (**A**) compared with MTX only (**B**). Inflamed synovium infiltrated with lymphocytes was found to contain abundant osteoclastic multinucleated cells on TRAP staining (**D** and **F**). However, there was no difference in metachromasia of articular cartilage in the left and right hind paws. **E,** Higher-magnification view of the boxed area in **C. F,** Higher-magnification view of the boxed area in **D.** Bo = subchondral bone; Ca = cartilage; Pa = pannus; S = synovial tissue (see Figure 1 for other definitions).

significantly and consistently increased from day 11 until the end of the experiment. However, in the M+/E+ group, swelling of the left hind paw was significantly suppressed on days 14, 18, and 21 (Figure 1B) when compared with the 3 control groups (M+/E−, M−/E+, and M−/E−). The gross appearance of the hind paws is shown in Figures 2A and B. Thus, application of electrical pulses appeared to prevent the hind paw joints from progressing to advanced AIA. The degree of swelling differed significantly between the left (electrically treated [EP+]) and right (EP−) paws of the same rat in the M+/E+ group (Figure 1C).

Radiologic evaluation of bones and joints. Radiologic analysis revealed that the hind paw joints were severely damaged in the M−/E−, M−/E+, and M+/E− groups at 21 days after injection of the adjuvant. Therefore, at a dose of 0.125 mg/kg body weight, MTX did not prevent the joint damage (Figure 2D) or local swelling (Figure 2B) caused by progression of arthritis. In contrast, the radiologic damage score was significantly lower in the electrically treated left (EP+) hind paws in the M+/E+ group (Figures 2A and C and Table 1).

Histologic analyses. In the M+/E+ group, the histologic scores were significantly lower in the left hind paws (EP+) than in the right hind paws (EP−) (Figures 3A and B and Table 1). Inflamed synovial tissues with abundant lymphocytes were observed to erode into subchondral bone (Figure 3B). In sections of these joints, the population of TRAP-positive multinucleated osteoclastic cells was significantly lower in the bones of the left hind paw (EP+) than in those of the right hind paw (EP−) (Figures 3C, D, E, and F and Table 1). Toluidine blue staining revealed no degenerative changes of cartilage tissue, including irregularity of articular surface, disorganization of tidemark, and alternation of metachromasia, in either hind paw (Figures 3G and H).

DISCUSSION

These results indicate positive effects of pulsed electrical stimulation for attenuating arthritis by enhancing the antiarthritic effect of MTX. We believe that this is attributable to micropores created by the electrical pulses in the cytoplasmic membranes of cells in the synovium or other inflamed cells. The subsequent passive influx of MTX into the cells would attenuate the inflammatory responses that led to the AIA, although this study did not provide direct evidence of MTX influx. In this preliminary study, we could not identify the cells targeted by electrochemotherapy, and MTX-negative synovial cells, inflammatory cells, or both, may be targets for the drug.

The effects of electrical fields on living cells have been investigated since the 1960s, and high-voltage electrical pulses have been reported to generate transient and reversible pores in cell membranes. This phenomenon has been termed electroporation and is currently used to transfer genes or drugs into cells (6). Electrochemotherapy involves electroporation with drugs, and this methodology is used for the treatment of malignant tumors (5–9). The use of electrochemotherapy to introduce anticancer drugs into malignant tumors has been reported, e.g., bleomycin

for melanoma, basal cell carcinoma, Kaposi's sarcoma, squamous cell carcinoma (6), or chondrosarcoma (15). However, electrochemotherapy with MTX for the treatment of RA has not been reported, although the less-permeable character of MTX and its use as a DMARD in RA would make it an ideal candidate for this approach. Because the effect of pulsed electrical stimulation is expected only at the local site, this method might be applicable for an isolated joint with arthritis that is refractory to systemic chemotherapy or in the early stages of RA involving a limited number of joints without significant joint-destructive changes.

Clinical application of this therapy should not affect normal tissues. Using TUNEL staining, we did not observed any difference in the number of apoptotic cells between the M+/E+ and M+/E− groups (data not shown). We also confirmed in the pilot study that electrical pulses, used under the same conditions as those used in this experiment, did not influence the normal tissues of inbred 9-week-old male Lewis rats. In this pilot study, no inflammatory reactions were observed on histologic examination of the area treated with the electrical pulses, suggesting that electroporation under these conditions did not cause any damage to normal tissue, including cartilage, bone, muscle, and blood vessels (results not shown). However, the clinical application of electrochemotherapy requires further study, including the dose of MTX and the parameters of the electrical pulses.

This experimental study is limited in 2 key areas. First, electrochemotherapy was not applied to joints with established arthritis, and the effect of electrochemotherapy was estimated based on the progression of arthritis. This differs from the clinical situation, in which, as indicated previously (10,11), the inflammatory phase in this AIA model is self-limiting. Therefore, the efficacy of electrochemotherapy for the treatment of established chronic arthritis is difficult to determine in this model. Second, optimization of the application of pulsed electrical current may not be sufficient to obtain maximum delivery of MTX into cells and to achieve maximal antiinflammatory effect in RA. The conditions that enable the efficacy of electrical stimulation in electrochemotherapy may be quite different from the conditions used in the clinical treatment of malignancies that were reference sources for the present study. The potential value of electrochemotherapy for the treatment of RA has been illustrated by these studies, and further work is required to optimize electrochemotherapy to control disease in joints with RA refractory to treatment.

REFERENCES

1. Maini R, St Clair EW, Breedveld F, Furst D, Kalden J, Weisman M, et al, and the ATTRACT Study Group. Infliximab (chimeric anti-tumour necrosis factor α monoclonal antibody) versus placebo in rheumatoid arthritis patients receiving concomitant methotrexate: a randomised phase III trial. Lancet 1999;354:1932–9.
2. Lipsky PE, van der Heijde DM, St Clair EW, Furst DE, Breedveld FC, Kalden JR, et al, and the Anti-Tumor Necrosis Factor Trial in Rheumatoid Arthritis with Concomitant Therapy Study Group. Infliximab and methotrexate in the treatment of rheumatoid arthritis. N Engl J Med 2000;343:1594–602.
3. Furst DE, Kremer JM. Methotrexate in rheumatoid arthritis. Arthritis Rheum 1988;31:305–14.
4. Multicenter evaluation of synovectomy in the treatment of rheumatoid arthritis: report of results at the end of three years. Arthritis Rheum 1977;20:765–71.
5. Heller R, Gilbert R, Jaroszeski MJ. Clinical applications of electrochemotherapy. Adv Drug Deliv Rev 1999;35:119–29.
6. Mir LM, Orlowski S. Mechanisms of electrochemotherapy. Adv Drug Deliv Rev 1999;35:107–18.
7. Hyacinthe M, Jaroszeski MJ, Dang VV, Coppola D, Karl RC, Gilbert RA, et al. Electrically enhanced drug delivery for the treatment of soft tissue sarcoma. Cancer 1999;85:409–17.
8. Horiuchi A, Nikaido T, Mitsushita J, Toki T, Konishi I, Fujii S. Enhancement of antitumor effect of bleomycin by low-voltage in vivo electroporation: a study of human uterine leiomyosarcomas in nude mice. Int J Cancer 2000;88:640–4.
9. Gothelf A, Mir LM, Gehl J. Electrochemotherapy: results of cancer treatment using enhanced delivery of bleomycin by electroporation. Cancer Treat Rev 2003;29:371–87.
10. Welles WL, Silkworth J, Oronsky AL, Kerwar SS, Galivan J. Studies on the effect of low dose methotrexate on rat adjuvant arthritis. J Rheumatol 1985;12:904–6.
11. Kawai S, Nagai K, Nishida S, Sakyo K, Murai E, Mizushima Y. Low-dose pulse methotrexate inhibits articular destruction of adjuvant arthritis in rats. J Pharm Pharmacol 1997;49:213–5.
12. Morgan SL, Baggott JE, Bernreuter WK, Gay RE, Arani R, Alarcon GS. MTX affects inflammation and tissue destruction differently in the rat AA model. J Rheumatol 2001;28:1476–81.
13. Clark RL, Cuttino JT Jr, Anderle SK, Cromartie WJ, Schwab JH. Radiologic analysis of arthritis in rats after systemic injection of streptococcal cell walls. Arthritis Rheum 1979;22:25–35.
14. Shiozawa S, Shimizu K, Tanaka K, Hino K. Studies on the contribution of c-fos/AP-1 to arthritic joint destruction. J Clin Invest 1997;99:1210–6.
15. Shimizu T, Nikaido T, Gomyo H, Yoshimura Y, Horiuchi A, Isobe K, et al. Electrochemotherapy for digital chondrosarcoma. J Orthop Sci 2003;8:248–51.

ARTHRITIS & RHEUMATISM
Vol. 52, No. 1, January 2005, pp 155–163
DOI 10.1002/art.20713

Use of Bone Morphogenetic Protein 2 and Diffusion Chambers to Engineer Cartilage Tissue for the Repair of Defects in Articular Cartilage

Masashi Nawata,[1] Shigeyuki Wakitani,[1] Hiroyuki Nakaya,[2] Akira Tanigami,[3] Toyokazu Seki,[3] Yukio Nakamura,[1] Naoto Saito,[1] Kenji Sano,[1] Eiko Hidaka,[1] and Kunio Takaoka[4]

Objective. **To examine the ability of cartilage-like tissue, generated ectopically in a diffusion chamber using recombinant human bone morphogenetic protein 2 (rHuBMP-2), to repair cartilage defects in rats.**

Methods. **Muscle-derived mesenchymal cells were prepared by dissecting thigh muscles of 19-day postcoital rat embryos. Cells were propagated in vitro in monolayer culture for 10 days and packed within diffusion chambers (10^6/chamber) together with type I collagen (CI) and 0, 1, or 10 μg rHuBMP-2, and implanted into abdominal subfascial pockets of adult rats. Tissue pellets were harvested from the diffusion chambers at 2 days to 6 weeks after implantation, and examined by histology, by reverse transcription–polymerase chain reaction (PCR) for aggrecan, CII, CIX, CX, and CXI, MyoD1, and core binding factor a1/runt-related gene 2, and by real-time PCR for CII. Tissue pellets generated in the chamber 5 weeks after implantation were transplanted into a full-thickness cartilage defect made in the patellar groove of the same strain of adult rat.**

Results. **In the presence of 10 μg rHuBMP-2, muscle-derived mesenchymal cells expressed CII messenger RNA at 4 days after transplantation, and a mature cartilage mass was formed 5 weeks after transplantation in the diffusion chamber. Cartilage was not formed in the presence of 1 μg rHuBMP-2 or in the absence of rHuBMP-2. Defects receiving cartilage engineered with 10 μg rHuBMP-2 were repaired and restored to normal morphologic condition within 6 months after transplantation.**

Conclusion. **This method of tissue engineering for repair of articular defects may preclude the need to harvest cartilage tissue prior to mosaic arthroplasty or autologous chondrocyte implantation. Further studies in large animals will be necessary to validate this technique for application in clinical practice.**

Regeneration of articular cartilage is a challenging subject for research on joint surgery (1), and several methods have been devised and attempted in clinical practice to repair focal defects in articular cartilage, especially in young patients (2–5). Currently, mosaic arthroplasty (6), a procedure in which pieces of autogeneic chondro-osseous mass are procured from peripheral parts of the joint surface and transplanted into the focal cartilage defects, is often used with success in the knee joint (7). However, a number of limitations persist, and these include the limited source of the autogeneic osteochondral tissue mass and the potential risk of progression to osteoarthritis due to the injury caused by procurement of graft tissue from the normal joint surface. In addition, the functional durability of the repaired cartilage and the limited application of the approach to small joints are further areas of concern.

Recently, technologies have been developed in order to fabricate tissues for the repair of skeletal defects. The transplantation of chondrocytes of auto- or allogeneic origin has been demonstrated in both experimental (8–11) and clinical (12) situations. In these

Supported in part by a Grant-in-Aid for Scientific Research from the Japanese Ministry of Education, Culture, Sports, Science and Technology (16390436).

[1]Masashi Nawata, MD, Shigeyuki Wakitani, MD, PhD, Yukio Nakamura, MD, Naoto Saito, MD, PhD, Kenji Sano, PhD, Eiko Hidaka, PhD: Shinshu University School of Medicine, Matsumoto, Japan; [2]Hiroyuki Nakaya, MD: Osaka University Medical School, Osaka, Japan; [3]Akira Tanigami, MD, PhD, Toyokazu Seki, PhD: Otsuka Pharmaceutical Company, Tokushima, Japan; [4]Kunio Takaoka, MD, PhD: Osaka City University Medical School, Osaka, Japan.

Address correspondence and reprint requests to Shigeyuki Wakitani, MD, PhD, Department of Orthopaedic Surgery, Shinshu University School of Medicine, 3-1-1 Asahi, Matsumoto 390-8621, Japan. E-mail: wakitani@hsp.md.shinshu-u.ac.jp.

Submitted for publication May 6, 2004; accepted in revised form September 14, 2004.

cases, cells are dissociated from pieces of articular cartilage, propagated (or left unpropagated) on dishes in ex vivo conditions to expand the cell population, and then transplanted with or without scaffolding carrier materials into the cartilage defect of the recipient. Although these methods can repair cartilage defects, some difficulties persist. Allogeneic transplantation has the inherent risks of disease transmission and rejection; autologous transplantation causes damage to the donor site.

In an effort to address the limitations of existing approaches, we attempted to generate cartilage tissue by inducing the differentiation of muscle-derived cells into the chondrocytic lineage in an in vivo environment with recombinant human bone morphogenetic protein 2 (rHuBMP-2). Articular defects in rat joints that received the induced cartilage-like tissue were repaired and restored to normal condition. The present report provides evidence to support this approach for the successful treatment of articular cartilage defects.

MATERIALS AND METHODS

Preparation of muscle-derived mesenchymal cells and diffusion chambers. Mesenchymal cells were obtained from the thigh muscles of 19-day, postcoital, F344 rat embryos (purchased from Japan SLC, Hamamatsu, Japan). The muscle tissues were minced with scissors and digested in 0.25% trypsin with 1 m*M* EDTA-Na_4 (Invitrogen, Carlsbad, CA). The dissociated cells were propagated on plastic culture dishes (10 cm in diameter) in Dulbecco's modified Eagle's medium (Invitrogen) supplemented with 10% (volume/volume) fetal calf serum (Invitrogen) and antibiotics (mixture of 5 mg/ml penicillin G, 5 mg/ml streptomycin, 10 mg/ml neomycin; Invitrogen) and passaged under routine culture conditions for 10 days. At the end of this period, the cells were detached from the dishes with 0.25% trypsin with 1 m*M* EDTA-Na_4 and packed within diffusion chambers (10^6 cells/chamber).

In order to construct a diffusion chamber for cell transplantation, a diffusion chamber kit (Millipore, Billerica, MA), consisting of a plastic ring (14 mm in outer diameter and 10 mm in inner diameter), a membrane filter (comprising a mixture of cellulose acetate and cellulose nitrate [0.45 μm in pore size]), and adhesive sealant, was utilized. The inner diameter of the ring was reduced to 5 mm by inserting another plastic ring. Only one side of the larger plastic ring was initially sealed with a membrane filter and adhesive sealant. For the next step, 40 μl of 0.3% (weight/weight) pig type I collagen (Cellmatrix LA; Nitta Gelatin, Osaka, Japan) and 0, 1, or 10 μg of rHuBMP-2 (Yamanouchi Pharmaceutical, Tokyo, Japan) were introduced into the diffusion chamber. The chamber was then freeze-dried and sterilized with ethylene oxide gas.

After these processes were completed, 10^6 cells suspended in 40 μl of serum-free culture medium containing 0.3% (w/w) pig type I collagen (Cellmatrix I-A; Nitta Gelatin) were introduced into the diffusion chamber, and another open side of the chamber was sealed with a filter and adhesive sealant. Sixty-two chambers (42 for histologic examination, 8 for reverse transcription–polymerase chain reaction [RT-PCR] analysis, and 12 for real-time PCR analysis) with 10 μg of rHuBMP-2 (group B10), 10 chambers (all for histologic examination) with 1 μg of rHuBMP-2 (group B1), and 46 chambers (26 for histologic examination, 8 for RT-PCR analysis, and 12 for real-time PCR analysis) without rHuBMP-2 (group B0) were prepared for analysis and implantation.

Transplantation of the diffusion chamber into the abdominal pocket of rats. Immediately after loading the cells into the diffusion chambers, each chamber was surgically inserted into a pocket in the abdominal muscles of 8-week-old F344 rats under diethyl ether anesthesia. After surgery, the rats were housed in cages and were given free access to standard chalk-like food and water. At 2, 4, 6, 8, 14, 21, 28, 35, and 42 days after implantation, the animals were killed in due order and the diffusion chambers were harvested (Table 1) for histologic examination. For RT-PCR analysis, 2 chambers were harvested at 2-, 4-, 7-, and 14-day intervals after implantation. For real-time PCR analysis, 2 chambers were harvested at 2-, 4-, 6-, 14-, 28-, and 42-day intervals after implantation.

Harvested tissue pellets within the chambers were inspected for vascular invasion caused by seal failure or breakage of the filter membranes. When vascular invasion was noted, the tissue was excluded from the transplantation into the cartilage defect and from PCR analysis. The tissue pellets for histologic examination were radiographed and fixed in 20% neutral buffered formalin solution, prior to processing for histologic examination. Some parts of the tissue pellet from the 5-week-old sample were used for transplantation into the rat-knee defect. Tissue pellets for RT-PCR or real-time PCR were frozen in liquid nitrogen immediately after harvesting.

Transplantation of tissue pellets from diffusion chambers into osteochondral defects of rats. Some portions of the tissue pellet removed from the diffusion chambers at 5 weeks after implantation were transplanted into cartilage defects generated on the patellar grooves of the knee joints of 7 (4 from group B10, 3 from group B0) mature, same-strain rats (a quarter tissue pellet/animal). The transplantation procedure was performed with the rats under anesthesia, using an intramuscular injection of a mixture of ketamin (100 mg/ml, 0.6

Table 1. Cartilage formation in diffusion chamber*

	rHuBMP-2			Area of cartilage tissue in cross-section
	0 μg	1 μg	10 μg	
2 days	0/2	–	0/2	–
4 days	0/2	–	0/2	–
6 days	0/2	–	0/2	–
8 days	0/2	–	0/2	–
14 days	0/2	–	0/2	–
21 days	0/4	–	4/6	1/4
28 days	0/4	0/4	9/10	1/3
35 days	0/4	0/6	9/10	Almost all
42 days	0/4	–	6/6	Almost all

* Except where indicated otherwise, values are the number of samples with cartilage formation/number of experiments. rHuBMP-2 = recombinant human bone morphogenetic protein 2.

ml/kg body weight; Sankyo, Tokyo, Japan) and xylazine (20 mg/ml, 0.3 ml/kg body weight; Bayel, Osaka, Japan). Pellets were transplanted into the left knees, and defects made on the right knees did not receive the implants.

In order to generate an osteochondral defect on the patellar groove of the distal femur of the rats, a longitudinal skin incision was made in the midline of the knee and the patellar groove was exposed by medial parapatellar arthrotomy and lateral dislocation of the patella. The osteochondral defect was made by drilling in 2 mm in depth and 2 mm in diameter, vertically to the patellar groove. The tissue pellet was detached from the inner surface of the membrane filters of the diffusion chamber and press-fitted into the defect. The knee joint was then closed with sutures. After surgery, the rats were fed in cages and killed at 24 weeks after surgery. The knee joints were excised and processed for histologic examination.

Histologic examination. Diffusion chambers and distal femurs with an articular cartilage defect were removed from the animals at 24 weeks after implantation and fixed in 20% buffered formalin. The harvested chambers were radiographed with a soft x-ray apparatus (Sofron, Tokyo, Japan) and visualized on radiographic films (Fuji Photo Film, Tokyo, Japan). The harvested chambers with calcified tissue and the distal ends of femurs with articular defects were decalcified in 4% EDTA solution, and then dehydrated with a gradient ethanol series, embedded in paraffin, sectioned in 5-μm thickness, and stained with hematoxylin and eosin or toluidine blue. Results of the histologic examination were evaluated using the scoring system described by Wakitani et al (13) for histologic grading of a cartilage defect (Wakitani's score; a lower score indicates improvement).

RT-PCR analysis. In order to detect changes in the expression of cartilage matrix–specific molecules in cells from the harvested diffusion chambers, RT-PCR analyses for aggrecan, types II, IX, X, and XI collagens, MyoD1, and core binding factor a1 (Cbfa1)/runt-related gene 2 (Runx2) were performed with the tissue pellets from the B10 and B0 groups. Frozen tissue pellets were ground down to powder with liquid nitrogen in a mortar on dry ice, and total messenger RNA (mRNA) was extracted from the tissue using TRIzol reagent (Invitrogen) according to the manufacturer's instructions. After treating samples with RNase-free deoxyribonuclease I (Takara Bio, Otsu, Japan), 500 ng of total mRNA from each sample was reverse transcribed using SuperScript II (Invitrogen). The reaction time was 60 minutes at 42°C. Thereafter, 1 μl of each reaction product was amplified in a 15-μl PCR mixture containing 0.5 units TaKaRa EX Taq (Takara Bio) and 10 pmoles of each primer to detect mRNA specific to each molecule.

Amplifications were performed in a Program Temp Control System (DNA Engine PTC-200; MJ Research, Waltham, MA) for 35 cycles after an initial denaturation step at 95°C for 3 minutes, denaturation at 95°C for 30 seconds, annealing for 30 seconds at 60°C, and extension at 72°C for 30 seconds, with a final extension at 72°C for 3 minutes. The PCR products (10 μl) were electrophoresed in a 3% agarose gel and detected by ethidium bromide staining. The nucleotide sequences of the primers for each of these genes are as follows: for AGC1, 5′-TCCAAACCAACCCGACAAT-3′ (forward) and 5′-TTCTGCCCAAGGGTTCTG-3′ (reverse); for Col2A1, 5′-GCTCGAGGAGACACTGGTG-3′ (forward) and 5′-ACCTGGGGGACCATCAGA-3′ (reverse); for Col9A1, 5′-GGTCCTCCGGGGAAGCCT-3′ (forward) and 5′-CCAACCTCTCCCGGCGGT-3′ (reverse); for Col10A1, 5′-CGAGGTCTTGTTGGCCCTAC-3′ (forward) and 5′-CCTGGGTCTCTGTCCGCT-3′ (reverse); for Col11A1, 5′-ATTGCCACCAGTCAACTGCT-3′ (forward) and 5′-TTGGACTGTGCCTCCGTC-3′ (reverse); for MyoD1, 5′-ACTACAGCGGCGACTCAGAC-3′ (forward) and 5′-GTGGAGATGCGCTCCACTAT-3′ (reverse); and for Cbfa1/Runx2, 5′-TGCTTCATTCGCCTCACAAAC-3′ (forward) and 5′-TAGAACTTGTGCCCTCTGTTG-3′ (reverse).

Real-time quantitative RT-PCR. Quantitative RT-PCR assay for type II collagen was carried out with the use of gene-specific expression–labeled fluorescent probes and sets of specific primers in an ABI PRISM 7700 sequence detection system (Applied Biosystems, Foster City, CA). On the basis of the published sequence of rat type II collagen, specific primer pair and probe sets were designed with the aid of Primer Express software, version 2.0 (Applied Biosystems). The sequences of the primers were 5′-AGGCGCTTCTGGTAACCCA-3′ (forward) and 5′-GACCAGTTGCACCTTGAGGAC-3′ (reverse), and the probe was 5′-TTCCCGGAGCCAAAGGATCTGCTG-3′. We used 6-carboxyfluorescein for type II collagen as the 5′ fluorescent reporter for the probe, while we added 6-carboxy-tetramethylrhodamine (Tamura Pharmaceutical, Osaka, Japan) to the 3′ end as a quencher.

Standard curves were constructed with the use of dilutions of accurately determined pCR2.1 plasmid vector (Invitrogen) containing complementary DNA (cDNA) products of type II collagen. A relative standard curve representing 10-fold dilutions of a rat type II collagen cDNA ranging from 2×10 to 2×10^5 copies/μl was used for linear regression analysis of the samples. PCR was carried out in 50 μl of reaction mixture containing 3 μl of the RT reaction, 1× Universal Master Mixture (Applied Biosystems), 500 n*M* of each primer, and 200 n*M* of the Taqman probe purchased from Applied Biosystems.

To compensate for the differences in cell number and/or RNA recovery, the copy number of type II collagen mRNA was determined relative to 18S ribosomal RNA (rRNA) (Applied Biosystems), which was also analyzed quantitatively. Thus, a partial cDNA of 18S rRNA was amplified from rat bone and cartilage samples using a specific primer set for 18S rRNA, and then subcloned into pCR2.1 (Invitrogen). Ten-fold dilutions of the resultant vector, pCR2.1-18S rRNA, ranging from 2×10 to 2×10^5 copies/μl, were used to construct a relative standard curve for 18S rRNA. The PCR mixture was basically the same as that for type II collagen, except for 200 n*M* of an 18S rRNA–specific Taqman probe set carrying a 5′-VIC reporter label and 3′-TAMURA quencher group, and 500 n*M* of the specific primer for 18S rRNA that was purchased from Applied Biosystems. These samples were placed in the ABI PRISM 7700 Sequence Analyzer and preheated at 95°C for 10 minutes, then amplified for 50 cycles of 95°C for 15 seconds, followed by 60°C for 1 minute. These experimental protocols were in compliance with the guidelines established by the Institutional Committee for Animal Care and Experiments of Shinshu University.

Statistical analysis. The histologic score was statistically analyzed using the SPSS software package (SPSS Japan, Tokyo, Japan). The Kruskal-Wallis H test followed by the

Mann-Whitney U test was used to determine differences between the groups.

RESULTS

Cartilage induction in diffusion chambers by rHuBMP-2. The tissue mass harvested from group B10 chambers (those receiving 10 μg rHuBMP-2) had a gelatinous appearance, with no histologic features characteristic of cartilage until 2 weeks after implantation. At 3 and 4 weeks after implantation, the tissue had a pale, opaque gelatinous appearance and revealed some cartilaginous characteristics along the inner surface of the filter membranes of the chamber on histologic examination (Figures 1A–H).

At 5 and 6 weeks postimplantation (Figures 1I–P), the cells of group B10 formed an elastic tissue mass with opaque appearance and no evidence of calcification on radiography (Figure 2B). Histologic examination of the opaque tissue mass in the chambers indicated normal features of cartilage, with round chondrocytic cells enclosed in a metachromatic matrix, as revealed by toluidine blue staining (Figures 1L and P). Small amounts of osseous tissue were found on the outer or host-side surfaces of the membrane filter of those samples. In one chamber with an accidental "hole" on the membrane filter, containing 5-week postimplantation tissue of group B10, the tissue became a hard mass with a reddish appearance; on radiography, the tissue was highly calcified (Figure 2C) and showed a normal histologic appearance of bone with hematopoietic marrow (Figure 2A). In contrast, the tissue of groups B0 (Figure 1) and B1 (chambers without rHuBMP-2 or with 1 μg rHuBMP-2, respectively) showed a gelatinous appearance with no histologic evidence of cartilage formation throughout the experimental period.

PCR findings. PCR analysis of the tissue in the diffusion chambers revealed a consistent expression of types X and XI collagen (Figure 3). Expression of type X collagen gradually increased in group B10. The expression of type II collagen was detected at low levels 2 days after implantation in group B10 (Figure 3). After 4 days, the expression of type II collagen was clearly detected in group B10. The expression of Cbfa1/Runx2 was clearly detected after 96

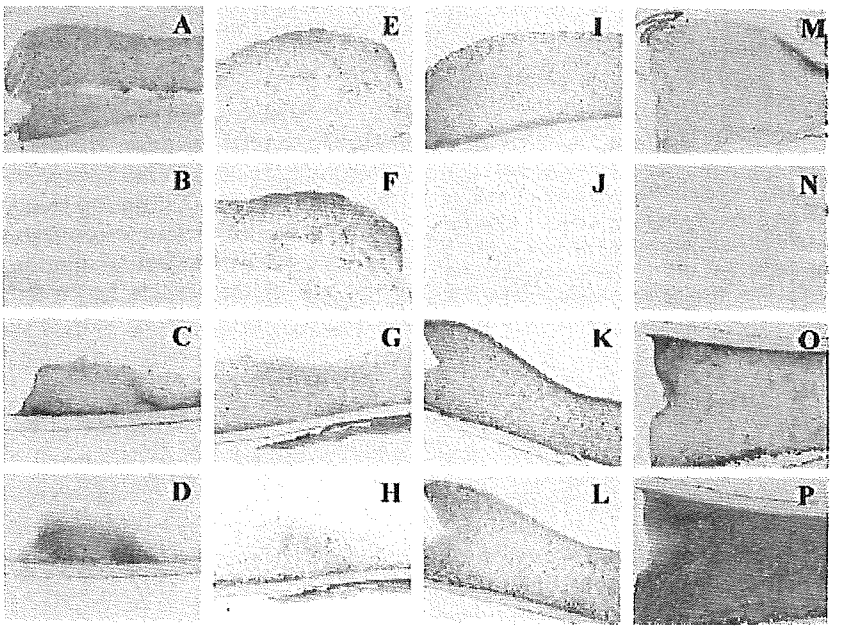

Figure 1. Cartilage formation in the diffusion chamber. Tissue pellets in diffusion chambers were examined at 3 weeks (**A–D**), 4 weeks (**E–H**), 5 weeks (**I–L**), and 6 weeks (**M–P**) postimplantation, in group B0 (without recombinant human bone morphogenetic protein 2 [rHuBMP-2]) (**A, B, E, F, I, J, M,** and **N**) compared with group B10 (with 10 μg rHuBMP-2) (**C, D, G, H, K, L, O,** and **P**). (Stained with hematoxylin and eosin in **A, C, E, G, I, K, M,** and **O**, with toluidine blue in **B, D, F, H, J, L, N,** and **P**; original magnification × 40.)

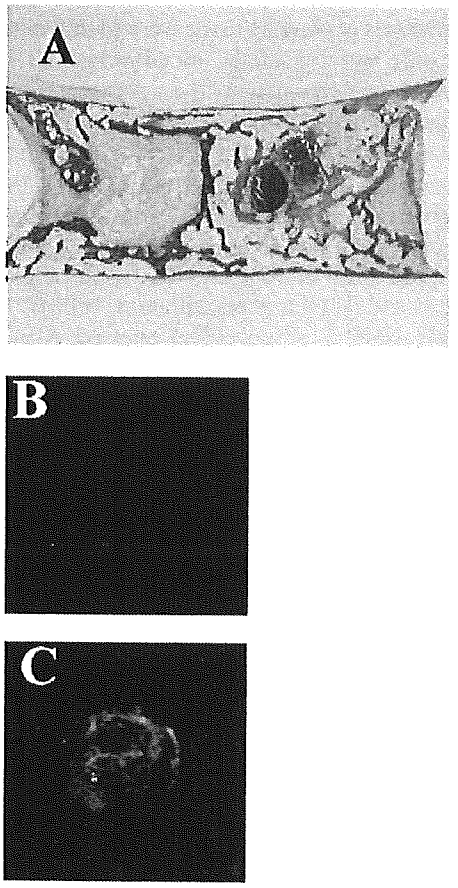

Figure 2. Histologic and radiologic evaluations of engineered cartilage tissue. For the tissue pellet in the diffusion chamber with an accidental hole on the filter (at 5 weeks posttransplantation; obtained from group B10), the normal histologic appearance of bone is clearly visible (stained with hematoxylin and eosin; original magnification ×20) (**A**), and the soft radiographic view shows bone trabeculae (**C**). Another soft radiographic view of group B10 tissue (same sample as in Figures 1K and L) shows no calcification (**B**).

hours in group B10 only (Figure 3). The expression of MyoD1 was not detected in either group at any time point.

Real-time PCR revealed that the expression of type II collagen increased markedly at 4 days after implantation (Figure 4). A high level of aggrecan was seen in group B10 after 2 days. Type IX collagen was weakly expressed in group B10 after 4 days, but increased significantly after 1 week. Low expression levels of aggrecan and type II collagen were detected in all groups at later time points in the study.

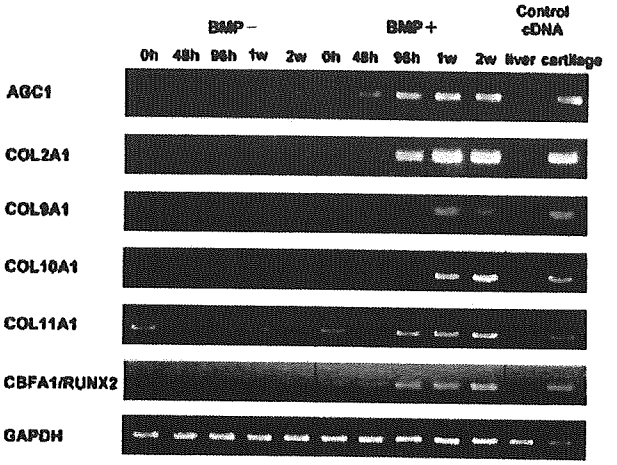

Figure 3. Reverse transcription–polymerase chain reaction analysis. Expression of types X and XI collagen (COL10A1 and COL11A1, respectively) was detected consistently in both groups (with 10 μg recombinant human bone morphogenetic protein 2 [BMP+; group B10] and without [BMP−]) throughout the experimental period. Expression of type IX collagen (COL9A1) was detected after 96 hours, indicating that effective cartilage matrix synthesis begins 3 or 4 days after implantation. Expression of type II collagen (COL2A1) was detected at low levels after 2 days in group B10 only, and after 4 days, it became more prominent. The expression of core binding factor a1/runt-related gene 2 (CBFA1/RUNX2) was clearly detected after 96 hours in group B10 only. AGC1 = aggrecan.

Repair of cartilage defects by transplantation of the engineered cartilage. The osteochondral defects that received the cartilaginous tissue mass, which was generated for 5 weeks in diffusion chambers containing tissue from group B10, were restored to a normal appearance at 24 weeks after transplantation. Upon examination, the site of the defects had a smooth surface and no

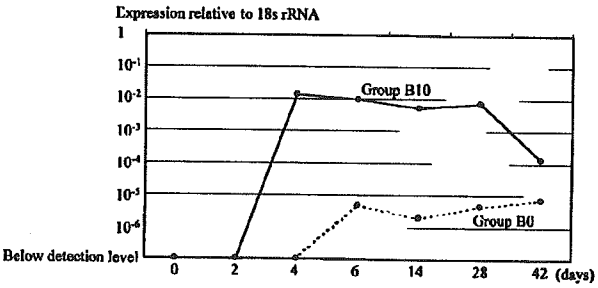

Figure 4. Real-time polymerase chain reaction analysis for type II collagen mRNA. After 4 days, expression of type II collagen mRNA was markedly increased in group B10 (with 10 μg recombinant human bone morphogenetic protein 2 [rHuBMP-2]). Group B0 = without rHuBMP-2; rRNA = ribosomal RNA.

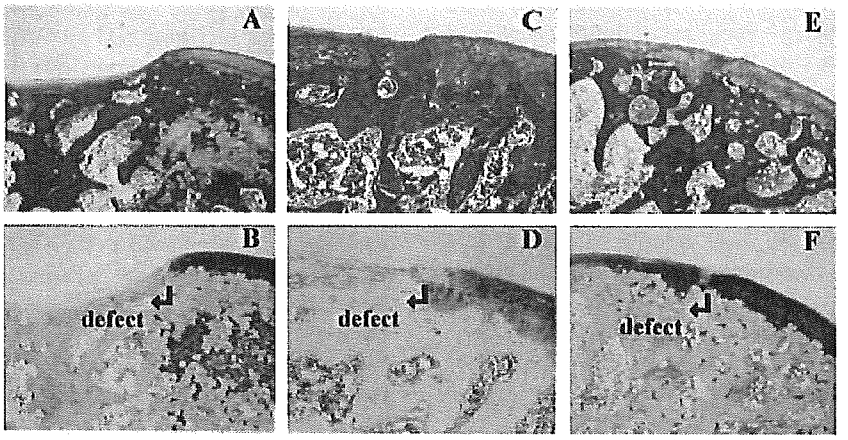

Figure 5. Osteochondral defects of a rat knee repaired with tissue pellets generated in diffusion chambers 24 weeks after transplantation. **A** and **B,** Defect with no implant. **C** and **D,** Defect implanted with tissue pellet generated in the chamber of group B0 (without recombinant human bone morphogenetic protein 2 [rHuBMP-2]). **E** and **F,** Defect implanted with tissue pellet generated in the chamber of group B10 (10 μg rHuBMP-2). (Stained with hematoxylin and eosin in **A, C,** and **E,** with toluidine blue in **B, D,** and **F**; original magnification × 40.)

obvious border with the surrounding normal articular cartilage (Figures 5E and F). The defects were filled with a layer of cartilage exhibiting subchondral cancellous bone connecting to the original subchondral bone. Although the architecture of the repaired articular cartilage was similar to that of normal cartilage with regard to cell arrangement, differences were noted. A tidemark was visible at the base of the cartilage layer adjacent to the subchondral bone, and the thickness of the regenerated cartilage was slightly less than that of the neighboring normal articular cartilage.

In contrast, the defects transplanted with tissue mass from group B0 were partially repaired, with a depressed surface visible at the defect site (Figures 5C and D). Histologic assessment of the defects that received either the tissue from group B0 or no implant revealed a small amount of fibrocartilage, with slightly positive metachromatic staining at the periphery of the defects and dominant fibrous tissue in the defect space.

Upon histologic evaluation of the knee cartilage after repair, the average histologic score (Wakitani's score) was 4.25 for group B10, 11.67 for group B0, and 14.00 for the defect-only group. The score for group B10 was significantly better than that for group B0 (P = 0.032) and the defect-only group (P = 0.002).

DISCUSSION

The experimental data presented herein indicate the capacity of rHuBMP-2 to induce the differentiation of young muscle-derived mesenchymal cells into chondrocytes within diffusion chambers in in vivo conditions. The resultant heterotopic cartilage formation represents a significant volume of induced tissue mass derived from these cells.

In order to induce the cartilage tissue, the diffusion chamber system was essential. When vascular invasion into the chamber occurred as a result of membrane seal failure, new bone with hematopoietic marrow was seen in the chambers harvested at 5 weeks after transplantation. Budenz and Bernard have reported similar findings (14). This bone was likely formed through the process of endochondral ossification, as deduced from classic reports describing the actions of BMP (15) and from comparison with the process of direct ossification (16,17). In the process of BMP-induced endochondral bone formation, cartilage is formed in the early phase of the bone-forming process. The cartilage tissue is then absorbed by invading vascular connective tissue and replaced by newly formed bone, as seen in embryonic osteogenesis (18) and in callus in fracture repair (19). During the process of ectopic bone formation elicited by

BMP, Tsuyama et al (20) found that the induced bone marrow cells are not the progeny of undifferentiated mesenchymal cells in situ, but rather arise from hematopoietic stem cells circulating in the peripheral blood. This conclusion was based on studies of chimeric mice and bone marrow transplantation (20).

In this diffusion chamber system, the cells within the chambers were able to survive by diffusion of tissue fluid from host animals, but vascular invasion was blocked by the filter membranes. As a result, the BMP-induced bone-forming reaction was stopped at the stage of cartilage formation and pieces of cartilage for transplantation were obtained, although it took a period of 5–6 weeks to achieve this outcome. This is a longer timeframe than the time taken by collagen pellets with rHuBMP-2 to form ectopic bone. In the ectopic endochondral bone formation process, ossification starts at the border of the cartilage and surrounding tissue.

The results of the RT-PCR analysis of type II collagen and aggrecan revealed that muscle-derived mesenchymal cells differentiated into chondrocytes at 4 days after implantation. However, mature cartilage matrix synthesis started a few days later, since the expression of type IX collagen, which is essential for type II collagen to form cartilage matrix, was weak at 4 days and increased significantly by day 7. Type X collagen and type XI collagen were detected by RT-PCR either with or without rHuBMP-2 in these cells. Because type II collagen and aggrecan were not detected initially, we cannot be sure that chondrogenesis started at the 0 time point. Further work will be needed to map out the exact sequence of expression of these genes in this model. In the absence of rHuBMP-2, the cells expressed type II collagen, but the level was much less when compared with that in cells with rHuBMP-2. This might mean that slow chondrogenesis of muscle-derived mesenchymal cells might occur even in the absence of rHuBMP-2 in this condition.

To examine whether osteogenic differentiation of the muscle-derived mesenchymal cells occurred in this system, we detected Cbfa1/Runx2, which is an essential transcriptional factor for osteoblastic differentiation, by RT-PCR. The expression of Cbfa1/Runx2 was observed at 96 hours in chambers with rHuBMP-2 but not observed in the absence of rHuBMP-2, which means that osteogenic differentiation was initiated by rHuBMP-2. We could not detect the expression of MyoD1 nor were there any cells showing a myogenic phenotype either in the chambers or in the defects at any time point.

The diffusion-chamber–engineered cartilage mass was able to repair full-thickness cartilage defects. At 24 weeks after transplantation, the transplanted cartilage was incorporated and effectively repaired the cartilage defects. The superficial layer of the transplant facing the joint surface had histologic characteristics of articular cartilage, but the greater part beneath the cartilage layer was replaced by bone mass, which was connected to the original subchondral bone. This morphologic condition suggests that part of the transplanted cartilage mass appeared to have features of preossifying cartilage and was in the process of remodeling. This adaptation to the surrounding environment also has been observed in an experiment involving cell transplantation to correct an osteochondral defect (13). When the cartilage plugs that were made in diffusion chambers were implanted into the osteochondral defects, they were replaced by bone from the bone marrow side, but the surface area that was in contact with the joint space remained as cartilage. We believe that the implanted chondrocytes remained at the surface of the defect, although there are no data to support this conclusion.

Adachi et al (21) reported that allogeneic muscle-derived cells embedded in collagen gels are useful for repair of full-thickness articular cartilage, both as a gene delivery vehicle and a cell source for tissue repair. They transduced rabbit allogeneic muscle-derived cells with the β-galactosidase gene (LacZ) and transplanted the cells into the osteochondral defects in the patellar groove in rabbit knees. They reported that the LacZ-positive cells were found in the defect only up to 4 weeks after transplantation. Further studies will be required to more completely understand the biochemical and morphologic processes that underpin the restorative actions of these cell and tissue transplants.

Although the generation of the new cartilage mass and repair of a cartilage defect with the engineered cartilage were shown to be successful in rats, there are some hurdles to be cleared before this approach can be applied in clinical practice. In this study, we used cells from the embryo, which were thought to be more primitive and to have greater capacity for differentiation. However, this represents a problem for clinical application, because of ethical and regulatory issues. Our technique could be applied to muscle-derived cells from the adult, and in this approach, we can use autologous cells. We are planning to apply this system to adult cells, such as bone marrow mesenchymal cells, adipocytes, and muscle-derived cells.

The less responsive nature of muscle-derived mesenchymal cells to rHuBMP-2 in large mammals, including humans, could also be an issue (22). Moreover, the optimal dose of BMP required for cartilage induc-

tion in humans must be determined. In order to solve these issues, further experimental studies in large animals will be essential.

The kinetics of BMP release from collagen is an important consideration. Sellers et al (23) reported that the mean residence time of rHuBMP-2 from a collagen sponge impregnated with 5 μg of rHuBMP-2 was 8 days, with an elimination half-life of 5.6 days. In addition, detectable amounts of rHuBMP-2 were present as long as 14 days after implantation.

In comparing the data from the present study with those reported by Sellers et al, there are differences in experimental details. Sellers et al implanted collagen with 5 μg of rHuBMP-2 into the osteochondral defect, which is likely to result in a rapid vascular invasion and much faster degradation. In the present study, collagen with 10 μg of rHuBMP-2 was placed into the chamber and implanted into subfascial pockets. The presence of the collagen in the chamber impeded invasion by the host cells. In addition, the preparation of a collagen gel and BMP-2 construct were different, and it would be reasonable to expect that the kinetics of BMP release would be influenced by these differences. It is also possible that the transplanted pellets might include BMP-2 at the time of implantation. Consequently, it would be the BMP-2, and not the cells in the pellet, that would drive the regeneration and the stability of repair cartilage. Further studies will be required to understand the kinetics of BMP release and the phenotypic stability of the transplanted cell population, which is believed to play a critical role in the outcome of tissue formation in vivo (24).

The present study has demonstrated another unique application of this approach, namely, the use of muscle-derived mesenchymal cells cultivated in an ex vivo system and differentiation of those cells into chondrogenic cells by rHuBMP-2 in diffusion chambers in an in vivo environment. Use of the muscle-derived mesenchymal cells together with rHuBMP-2 might be a reason for the successful generation of cartilage in this study, because these cells are known to have multilineage differentiation potential (21,25–27). While the present report provides evidence to support this approach for the successful treatment of articular cartilage defects, further studies will be needed to validate the technique for application in clinical practice.

REFERENCES

1. Buckwalter JA, Mankin HJ. Articular cartilage repair and transplantation. Arthritis Rheum 1998;41:1331–42.
2. Pridie KH. A method of resurfacing osteoarthritic knee joints. J Bone Joint Surg Br 1959;41:618–9.
3. Bert JM. Role of abrasion arthroplasty and debridement in the management of osteoarthritis of the knee. Rheum Dis Clin North Am 1993;19:725–39.
4. Steadman JR, Rodkey WG, Rodrigo JJ. Microfracture: surgical technique and rehabilitation to treat chondral defects. Clin Orthop 2001;391 Suppl:S362–9.
5. Hunziker EB. Articular cartilage repair: basic science and clinical progress [a review of the current status and prospects]. Osteoarthritis Cartilage 2002;10:432–63.
6. Matsusue Y, Yamamuro T, Hama H. Arthroscopic multiple osteochondral transplantation to the chondral defect in the knee associated with anterior cruciate ligament disruption. Arthroscopy 1993;9:318–21.
7. Jakob RP, Franz T, Gautier E, Mainil-Varlet P. Autologous osteochondral grafting in the knee: indication, results, and reflections. Clin Orthop 2002;401:170–84.
8. Chesterman PJ, Smith AU. Homotransplantation of articular cartilage and isolated chondrocytes: an experimental study in rabbits. J Bone Joint Surg Br 1968;50:184–97.
9. Grande DA, Pitman MI, Peterson L, Menche D, Klein M. The repair of experimentally produced defects in rabbit articular cartilage by autologous chondrocyte transplantation. J Orthop Res 1989;7:208–18.
10. Wakitani S, Kimura T, Hirooka A, Ochi T, Yoneda M, Yasui N, et al. Repair of rabbit articular surfaces with allograft chondrocytes embedded in collagen gel. J Bone Joint Surg Br 1989;71:74–80.
11. Kawamura S, Wakitani S, Kimura T, Maeda A, Caplan AI, Shino K, et al. Articular cartilage repair: rabbit experiments with a collagen gel-biomatrix and chondrocytes cultured in it. Acta Orthop Scand 1998;69:56–62.
12. Brittberg M, Lindahl A, Nilsson A, Ohlsson C, Isaksson O, Peterson L. Treatment of deep cartilage defects in the knee with autologous chondrocyte transplantation. N Engl J Med 1994;331:889–95.
13. Wakitani S, Goto T, Pineda SJ, Young RG, Mansour JM, Caplan AI, et al. Mesenchymal cell-based repair of large, full-thickness defects of articular cartilage. J Bone Joint Surg Am 1994;76:579–92.
14. Budenz RW, Bernard GW. Osteogenesis and leukopoiesis within diffusion-chamber implants of isolated bone marrow subpopulations. Am J Anat 1980;159:455–74.
15. Reddi AH. Cell biology and biochemistry of endochondral bone development. Coll Relat Res 1981;1:209–26.
16. Sasano Y, Ohtani E, Narita K, Kagayama M, Murata M, Saito T, et al. BMPs induce direct bone formation in ectopic sites independent of the endochondral ossification in vivo. Anat Rec 1993;236:373–80.
17. Kuboki Y, Saito T, Murata M, Takita H, Mizuno M, Inoue M, et al. Two distinctive BMP-carriers induce zonal chondrogenesis and membranous ossification, respectively; geometrical factors of matrices for cell-differentiation. Connect Tissue Res 1995;32:219–26.
18. Kronenberg HM. Developmental regulation of the growth plate. Nature 2003;423:332–6.
19. McKibbin B. The biology of fracture healing in long bones. J Bone Joint Surg Br 1978;60-B:150–62.
20. Tsuyama K, Takaoka K, Kitamura Y, Ono K. Origin of the marrow cells in bones induced by implantation of osteosarcoma-derived bone-inducing factor in mice. Clin Orthop 1983;172:251–6.
21. Adachi N, Sato K, Usas A, Fu FH, Ochi M, Han CW, et al. Muscle derived, cell based ex vivo gene therapy for treatment of full thickness articular cartilage defects. J Rheumatol 2002;29:1920–30.
22. Kawasaki K, Aihara M, Honmo J, Sakurai S, Fujimaki Y, Saka-

moto K, et al. Effects of recombinant human bone morphogenetic protein-2 on differentiation of cells isolated from human bone, muscle, and skin. Bone 1998;23:223–31.
23. Sellers RS, Zhang R, Glasson SS, Kim HD, Peluso D, D'Augusta DA, et al. Repair of articular cartilage defects one year after treatment with recombinant human bone morphogenetic protein-2 (rhBMP-2). J Bone Joint Surg Am 2000;82:151–60.
24. De Bari C, Dell'Accio F, Luyten FP. Failure of in vitro-differentiated mesenchymal stem cells from the synovial membrane to form ectopic stable cartilage in vivo. Arthritis Rheum 2004;50: 142–50.
25. Qu Z, Balkir L, van Deutekom JC, Robbins PD, Pruchnic R, Huard J. Development of approaches to improve cell survival in myoblast transfer therapy. J Cell Biol 1998;142:1257–67.
26. Lee JY, Qu-Petersen Z, Cao B, Kimura S, Jankowski R, Cummins J, et al. Clonal isolation of muscle-derived cells capable of enhancing muscle regeneration and bone healing. J Cell Biol 2000;150:1085–100.
27. Williams JT, Southerland SS, Souza J, Calcutt AF, Cartledge RG. Cells isolated from adult human skeletal muscle capable of differentiating into multiple mesodermal phenotypes. Am Surg 1999;65:22–6.

Eur Spine J (2005) 14 : 90–94
DOI 10.1007/s00586-004-0711-7

ORIGINAL ARTICLE

Orso L. Osti
Richard T. Gun
George Abraham
Nicole L. Pratt
Goran Eckerwall
Hiroaki Nakamura

Potential risk factors for prolonged recovery following whiplash injury

Received: 31 May 2003
Revised: 16 January 2004
Accepted: 4 March 2004
Published online: 25 May 2004

Study conducted at the University of Adelaide

O. L. Osti · G. Abraham · G. Eckerwall
Department of Orthopaedic Surgery and Trauma, The Queen Elizabeth Hospital, Woodville, Australia

R. T. Gun (✉) · N. L. Pratt
Department of Public Health, University of Adelaide, SA 5005 Adelaide, Australia
e-mail: richard.gun@adelaide.edu.au

H. Nakamura
Department of Orthopaedic Surgery, Osaka City University Medical School, Osaka, Japan

Present address:
G. Abraham
Department of Orthopaedic Surgery and Trauma, Christian Medical College, Velore, India

Abstract A retrospective analysis of insurance data was made of 600 individuals claiming compensation for whiplash following motor vehicle accidents. Three hundred randomly selected claimants who had settled their injury claims within 9 months of the accident were compared with 300 who had settled more than 24 months after the accident. We compared the two groups to identify possible risk factors for prolonged recovery, for which settlement time greater than 24 months was a marker. Variables considered included demographic factors, type of collision, degree of vehicle damage, workers compensation, prior claim or neck disability, treatment and time to settlement. Consulting a solicitor was associated with a highly significant, four-fold increase of late settlement of the claim. A concurrent workers' compensation claim, prior neck disability and undergoing physiotherapy or chiropractic treatment were weakly associated with late settlement. The degree of damage to the vehicle (as indicated by cost of repairs) was not a significant predictor of late settlement. Late settlement may be the direct effect of legal intervention, independent of the severity of the injury. Whilst the financial benefit to the claimant of consulting a solicitor is apparent, the benefit of prolonged disability is not. It may be to the advantage of both insurers and claimants if those likely to proceed to late settlement could be recognised early and their claims settled expeditiously.

Keywords Whiplash · Neck injury · Motor vehicle accident · Compensation claim · Legal representation

Introduction

Whiplash is a common injury. In South Australia approximately 4,000 claims for whiplash, at a cost of the order of Australian $50 million, are made annually (for a population of 1.5 million). There is some evidence that the incidence of this condition has increased in recent decades, although it appears unrelated to increased seat belt use [11].

In an extensive review, the Quebec Task Force (QTF) on whiplash-associated disorders has noted that cases are usually self-limited, with a median time to recovery – measured by time to the end of disability compensation – of 31 days. However, a significant fraction exhibited prolonged disability: 10% of the cases studied in the Quebec cohort study were still unable to resume normal activity 200 days post-injury [8]. In a review of studies published since the QTF report, considerable variation has been found in the duration and extent of recovery. Important sources of variation have been the outcome measures used (e.g., settlement of claim, return to work, persistence of symptoms) and the type of insurance system (e.g., tort or no-fault) [3].

It is unclear if protracted disability from whiplash is related to the degree of trauma. In a 1996 review of whi-